

## THEORETICAL STUDIES ON THE HYDROLYSIS OF UREA IN ACID SOLUTION<sup>1</sup>

IKCHOON LEE\* AND CHANG KON KIM

*Department of Chemistry, Inha University, Incheon, 420-751, Korea*

and

BYUNG CHOON LEE

*Department of Chemistry, Choongbuk National University, Chongju, 360-763, Korea*

### ABSTRACT

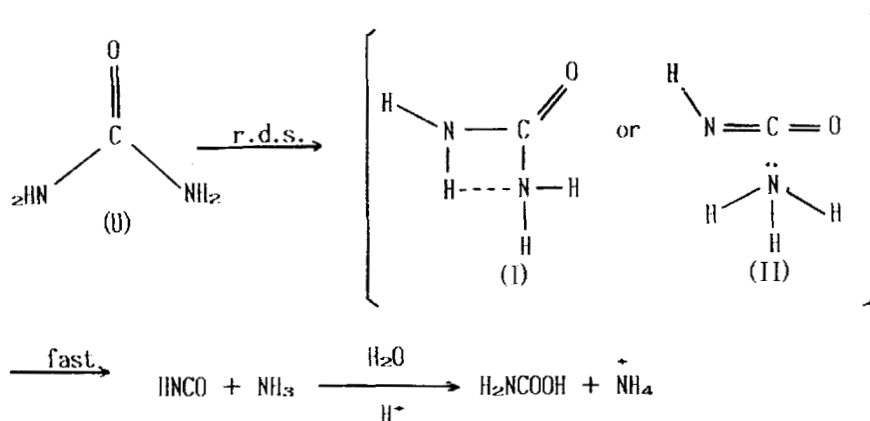
Mechanisms of the hydrolysis of urea have been investigated using the MNDO and AM1 methods. All geometries were fully optimized and the transition states were characterized by calculating force constants. The results showed that: (i) The unimolecular decomposition process via the direct intramolecular proton transfer is preferred to both the A1 and the bimolecular nucleophilic attack by water, in agreement with the experimental results of Shaw *et al.* in the low acidity medium. (ii) The diprotonated form of urea exists as an equilibrium species, which undergoes the A2 type hydrolysis more favorably than the monoprotinated form, as Moodie *et al.* found in the intermediate acidity medium. (iii) The A2 hydrolysis of the monoprotinated form is very similar to those of acetamide and methyl carbamate. (iv) As the number of the solvate water molecules increases, the activation barrier for the A2 process of the monoprotinated form increases while that for the unimolecular decomposition of the free base form decreases, indicating a possibility of the barrier height reversal in the bulk solvent in favor of the latter process, thus accommodating all the experimentally found trends in the urea hydrolysis. The A1 mechanisms involving six-membered ring type intermediates can be ruled out as untenable since no such equilibrium species was obtained by both the MNDO and AM1 calculations.

Ureas have been widely studied experimentally in view of their biochemical and chemical importance. However, no consensus of opinion has yet been established as to the mechanism of their hydrolysis in acid solution. Shaw *et al.*<sup>2</sup> have shown that the hydrolysis of urea in dilute acid solution does not involve acid catalysis but decomposition via intramolecular hydrogen transfer and dissociation of the transition state (TS), (I) or (II), as in Scheme 1.

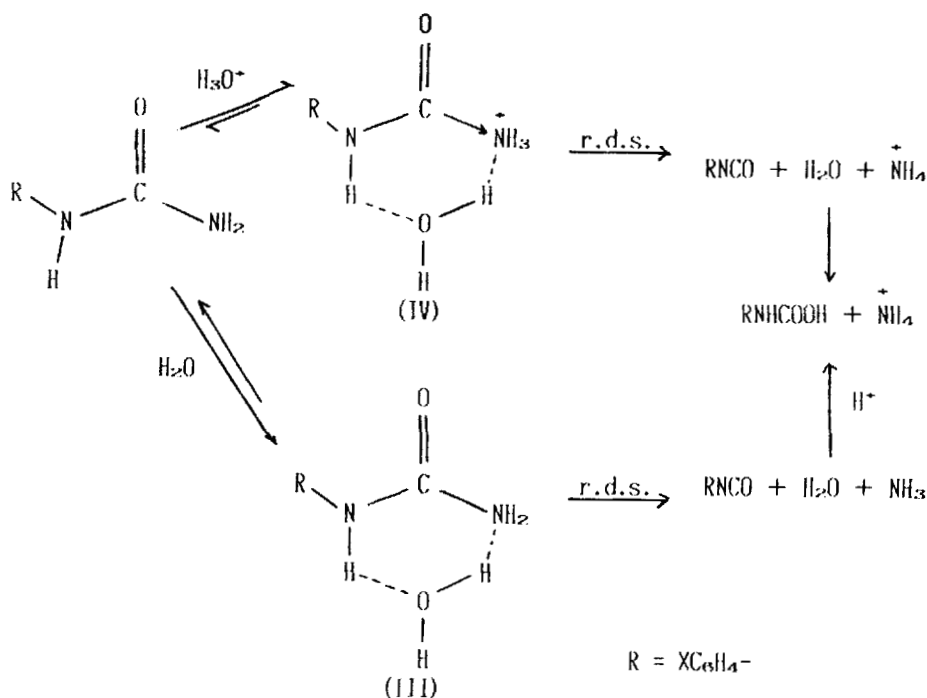
Moodie *et al.*<sup>3</sup> have argued further that the decrease in observed rate constants with the increase in acid concentration is due to a decrease in concentration of the free base, (U), and a shallow maximum found in the more concentrated acidity range, ca. 70% w/w H<sub>2</sub>SO<sub>4</sub>, can be attributed to the A2 hydrolysis of the diprotonated form, UH<sub>2</sub><sup>2+</sup>. On the other hand, Giffney *et al.*<sup>4</sup> have proposed a different mechanism of hydrolysis for phenylureas (XC<sub>6</sub>H<sub>4</sub>NHCONH<sub>2</sub>) in which water acts as a proton transfer agent to either the unprotonated, (III), or the minor N-protonated conjugated acid, (IV), prior to the rate determining decomposition as shown in Scheme 2.

---

\*Author for correspondence.



Scheme 1



Scheme 2

In previous papers of this series of semi-empirical MO studies on the acid hydrolysis of amides and related compounds, one of the questions we have addressed was whether there is a common mechanism for the acid hydrolysis of amides, carbamates and ureas. Our MNDO studies on the mechanism of the acid hydrolysis of acetamide<sup>5</sup> and methyl carbamate<sup>6</sup> have indeed shown that the two proceed through a common mechanism involving two steps; (i) the rate determining nucleophilic attack of the carbonyl carbon of the N-protonated tautomer by water, and (ii) the fast subsequent proton abstraction by the leaving group,  $\text{NH}_3$ , to form products.

In this work we examine the hydrolysis mechanism of urea in acid solution theoretically using the MNDO<sup>7</sup> and AM1<sup>8</sup> methods. We have explored all the experimentally postulated mechanisms, and the solution phase behavior was deduced from the effect of increasing number of solvate water molecules on barrier heights for the hydrolysis of neutral and protonated urea.

### CALCULATIONS

The calculations were carried out using the standard MNDO<sup>9a</sup> and AM1<sup>9b</sup> procedures with full optimization of all geometric variables. Transition states (TS) were located by the reaction coordinate method,<sup>10</sup> refined with the gradient norm minimization method<sup>11</sup> and characterized by confirming only one negative eigenvalue in the Hessian matrix.<sup>12</sup> In the solvent effect studies, the geometries of the ground states and TSs were fixed and the structures of attached solvate water molecules only were optimized.

### RESULTS AND DISCUSSION

#### Hydrolysis of the free base

Three processes are conceivable for the hydrolysis of the free base:

##### (i) Intramolecular decomposition of urea through the TS (I) or (II) in Scheme 1

In this process, intramolecular 1,3-hydrogen transfer of an N-bound hydrogen to N' atom takes place within the neutral urea, (U), in the rate determining step with dissociation of the

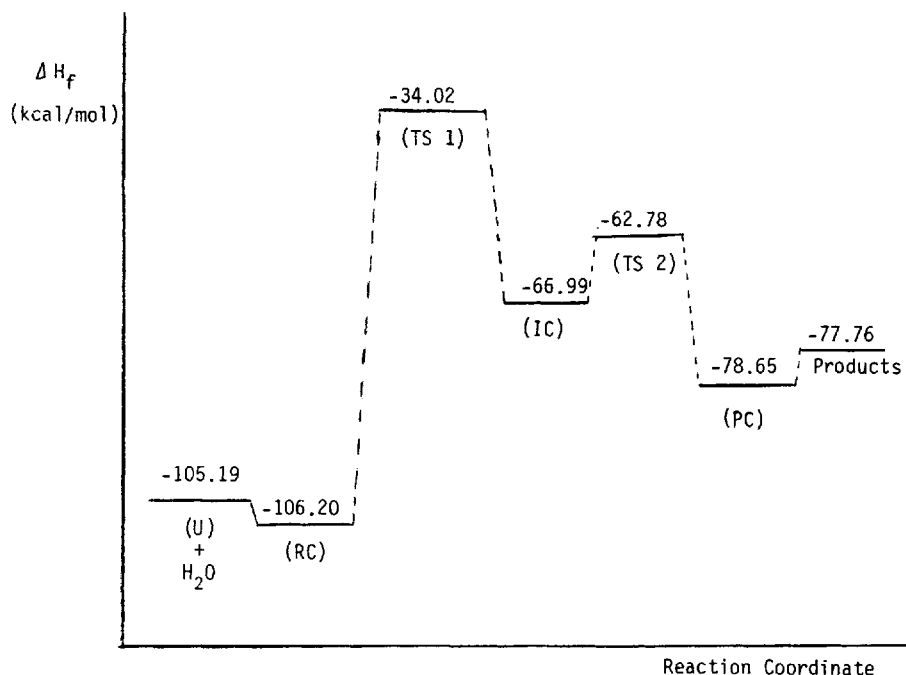


Figure 1. Potential energy profile for the intramolecular decomposition process of neutral urea, (U) + H<sub>2</sub>O

TS into  $\text{NH}_3$  and  $\text{HNCO}$ , which reacts further with water to form carbamic acid,  $\text{H}_2\text{NCOOH}$ . The potential energy profile and the optimized structures of the stationary point species by the MNDO calculations are presented in Figures 1 and 2. Inspection of Figure 1 shows that a typical 1,3-hydrogen transfer<sup>13</sup> between N atoms through the 4-membered cyclic TS is the rate determining step with an activation barrier of 71.17 kcal/mol. We note that the TS corresponds to (I), not to (II), in Scheme 1, the latter being actually a metastable intermediate (IC) on the potential energy surface. This is consistent with Werner's proposal<sup>14</sup> that the structure (II) is an intermediate formed by a simple nucleophilic attack of  $\text{HNCO}$  by  $\text{NH}_3$  in the reverse reaction of the urea decomposition process.<sup>15</sup> The complex IC decomposes into  $\text{HNCO}$  and  $\text{NH}_3$  through the TS 2 which is much lower (by  $\sim 30$  kcal/mol) than the TS 1. Experimentally the rest of the reaction is known to proceed rapidly in solution phase.<sup>2</sup>

The AM1 calculations on this process gave similar stationary point structures with the lower activation barrier by 11.32 kcal/mol compared to that by the MNDO method (*vide infra*). This is an expected trend<sup>16</sup> since MNDO is known to overestimate activation barriers.<sup>8,17</sup>

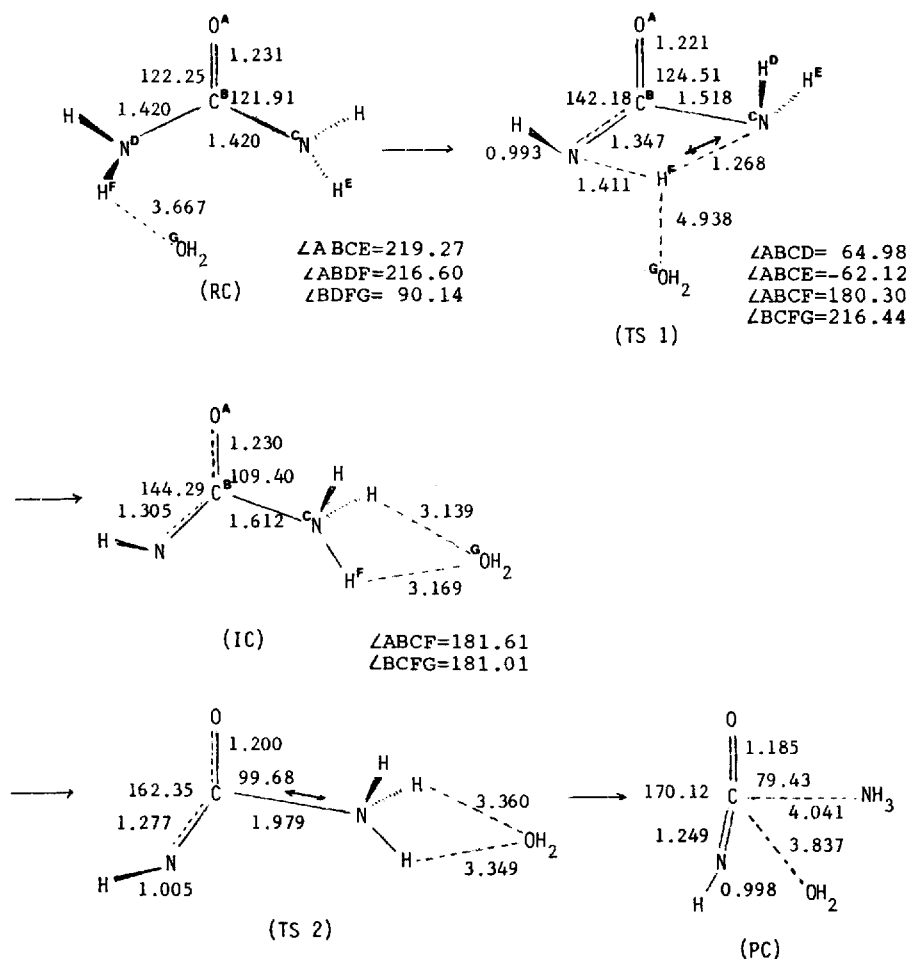


Figure 2. Geometries for the stationary point species on the potential energy profile for the intramolecular decomposition process. The double headed arrow ( $\leftrightarrow$ ) indicates a reaction coordinate and the dihedral angle is represented with the  $\text{LWXYZ}$  (bond lengths and angles are in Å and degree)

(ii) *Intermolecular decomposition of  $U \cdot H_2O$  in Scheme 2*

In the process proposed by Giffney *et al.*<sup>4</sup> (Scheme 2), water is supposed to act as a hydrogen transfer agent in a stable six-membered cyclic complex, (III), which decomposes in the rate determining step. Our attempts at the geometry optimization with both the MNDO and AM1 methods, however, failed to give a stationary state corresponding to the six-membered cyclic complex, (III). We have nevertheless proceeded with the AM1 calculations and obtained a reactant complex (RC) resembling the corresponding complex in the intramolecular decomposition process, Figure 2. The six-membered cyclic structure, (III), was in fact obtained as the TS with the activation barrier of 60.85 kcal/mol, preceding an intermediate complex (IC) formation from the RC. Our AM1 results showed that the overall processes for the intramolecular (Scheme 1) and the intermolecular decompositions (Scheme 2 with  $R = H$ ) of the free base are similar except the TS structure and the barrier height; the barrier height is lower in the former by *ca.* 1 kcal/mol than in the latter process. Thus the two processes of the free urea decomposition may compete in practice, since the difference in the activation barrier is only marginal. The potential energy profiles and the stationary point structures for the two processes calculated by the AM1 method are shown in Figures 3 and 4, respectively.

(iii) *Direct nucleophilic attack of urea by water at the carbonyl carbon*

In this process, the rate determining nucleophilic attack of the carbonyl carbon by water proceeds with concurrent transfer of a hydrogen atom from  $H_2O$  to the carbonyl oxygen forming a gem-diol, (V), in Scheme 3. One of the hydrogen atoms in the diol is then transferred to N atom via the 1,3-hydrogen shift, and the rest of the reaction follows as in (i).

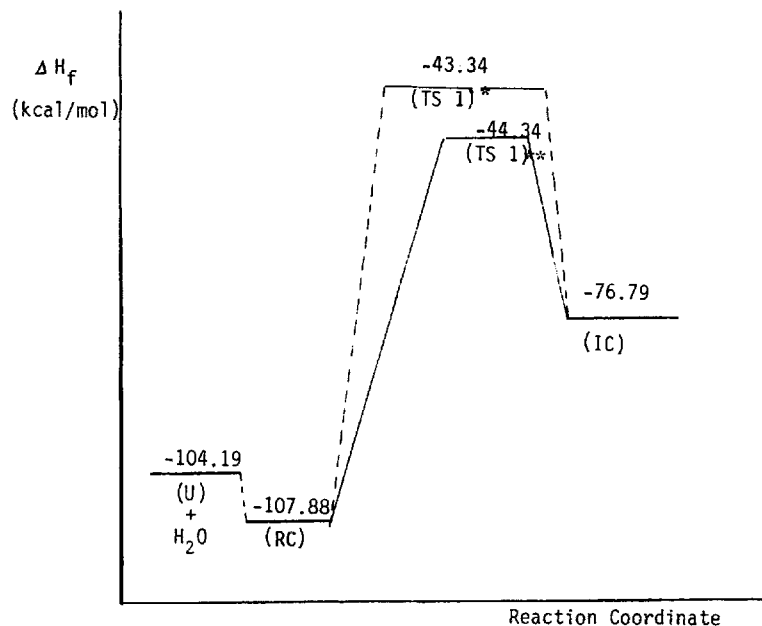


Figure 3. Potential energy profile for the intramolecular and intermolecular decomposition processes of neutral urea, (U) +  $H_2O$ . \* is an intermolecular decomposition process and \*\* is an intramolecular process. These results are obtained by AM1 method

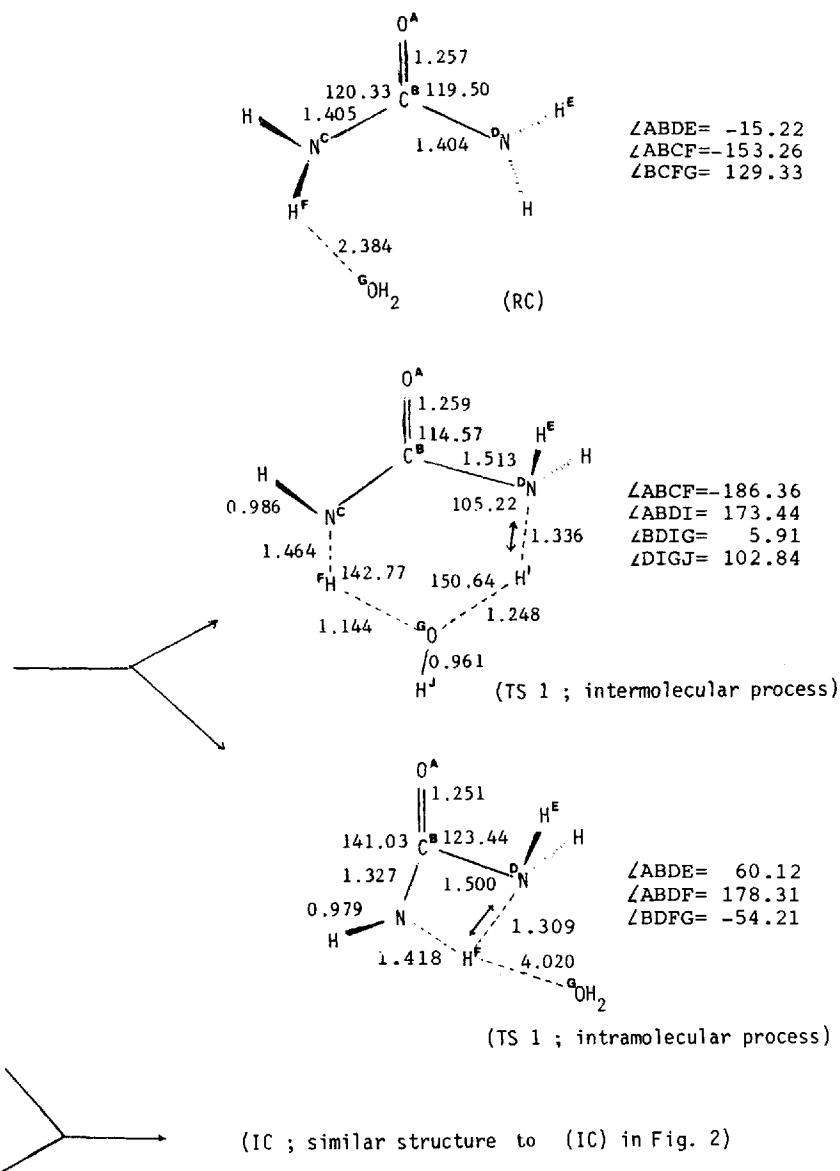
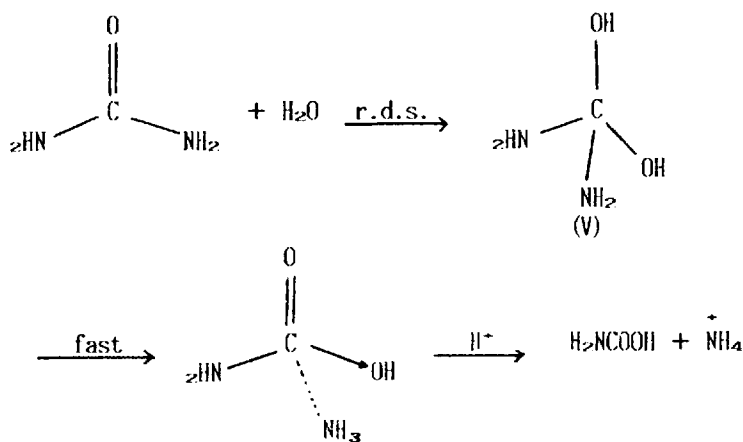


Figure 4. Some geometries for the stationary point species on the potential energy profile for the intramolecular and intermolecular decomposition process of neutral urea. The double headed arrow ( $\leftrightarrow$ ) indicates a reaction coordinate and the dihedral angle is represented with the  $\angle WXYZ$  (bond lengths and angles are in Å and degree)

The MNDO potential energy profile and the optimized geometries of stationary point structures are presented in Figures 5 and 6. The activation barrier for this process was found to be 78.27 kcal/mol by the MNDO method, which is 7.10 kcal/mol higher than the MNDO barrier for process (i). This is consistent with the experimental results of Shaw *et al.*<sup>2</sup> that the hydrolysis of neutral urea occurs mainly by the intramolecular decomposition path, (i).



Scheme 3

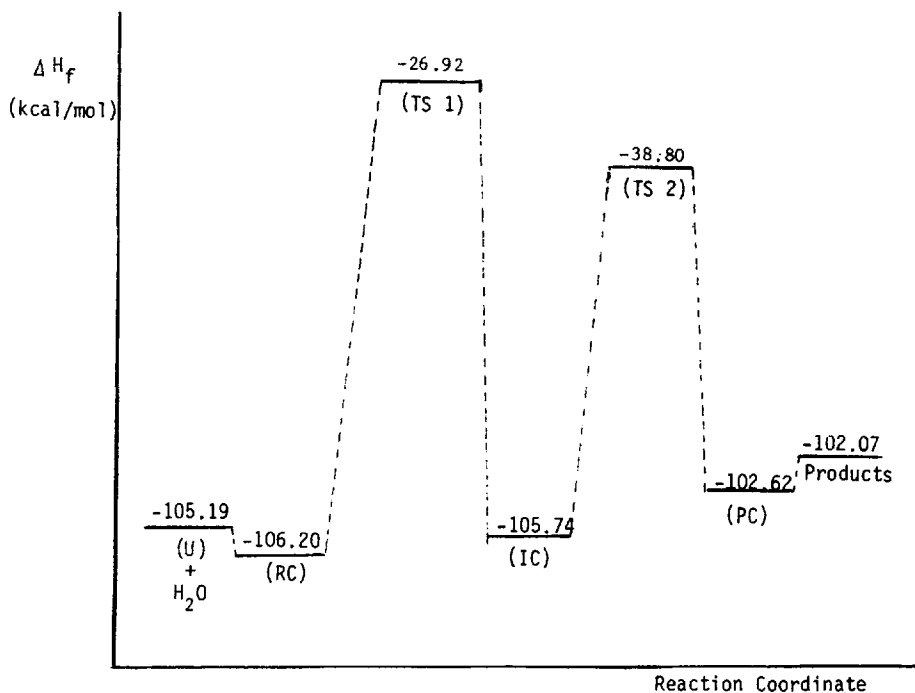


Figure 5. Potential energy profile for the direct nucleophilic attack of neutral urea by water at the carbonyl carbon, (U) + H<sub>2</sub>O

### Hydrolysis of the monoprotonated urea

In the moderate acid solution, two monoprotonated tautomers, the O-protonated (VI) and N-protonated (VII), will be in equilibrium (process 1 in Scheme 4), and the acid hydrolysis is therefore possible from either one of the two forms (processes 2 and 3 in Scheme 4).

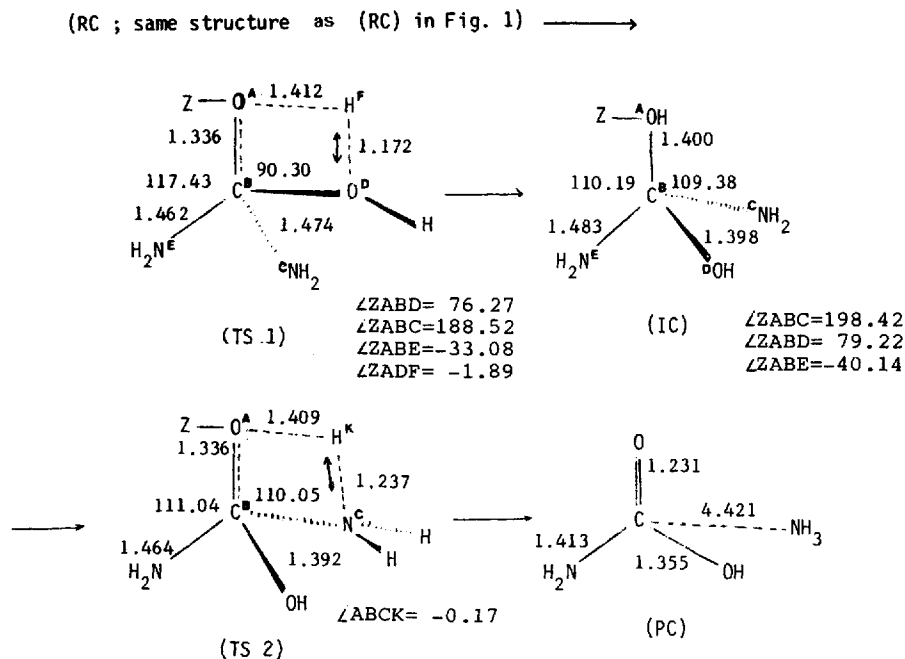
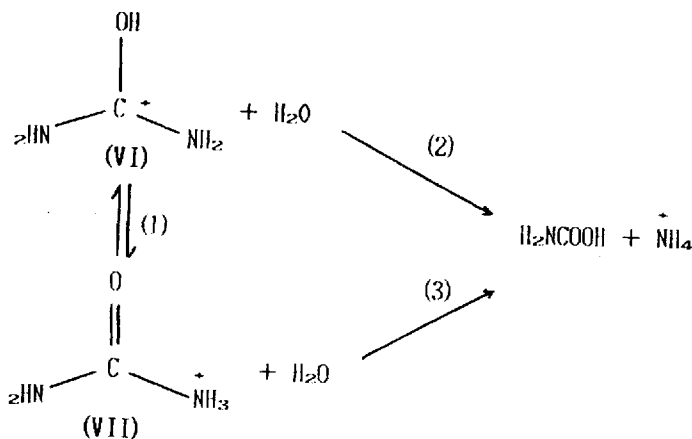


Figure 6. Geometries for the stationary point species on the potential energy profile for the direct nucleophilic attack of neutral urea by water at the carbonyl carbon. The double headed arrow ( $\longleftrightarrow$ ) indicates a reaction coordinate and the dihedral angle is represented with the  $\angle WXYZ$ . The Z is a dummy atom (bond lengths and angles are in Å and degree)

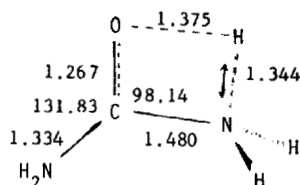


Scheme 4

The proton transfer equilibrium (1) is quite similar to those in acetamide and methyl carbamate;<sup>18</sup> the gas phase transfer involves a typical intramolecular 1,3-proton shift with a high activation barrier of 70-20 kcal/mol, whereas participation of one solvate water changes the process to go through in an intermolecular manner with substantial lowering of the MNDO activation barrier (by 39-33 kcal/mol). The optimized TS geometries by the MNDO method for the two proton transfer processes are shown in Figure 7.



(a) TS for the gas phase proton transfer, (VI)  $\rightarrow$  (VII).



(b) TSs for the solvated proton transfer, (VI) + H<sub>2</sub>O  $\rightarrow$  (VII) + H<sub>2</sub>O.

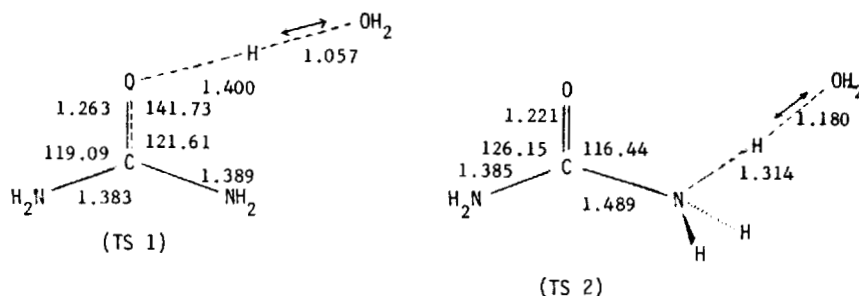


Figure 7. TS geometries for the two proton transfer processes. The double headed arrow ( $\leftrightarrow$ ) indicates a reaction coordinate (bond lengths and angles are in Å and degree)

The A2 hydrolysis of the O-protonated form (VI) is again similar to those of the O-protonated acetamide<sup>5</sup> and methyl carbamate.<sup>6</sup> The MNDO activation barrier found for process (2) was 59.83 kcal/mol, which is somewhat higher than those of acetamide (51.72 kcal/mol) and methyl carbamate (51.74 kcal/mol). Some of the optimized geometries and the potential energy profile are presented in Figures 8 and 9.

The hydrolysis of the N-protonated tautomer, process (3) in Scheme 4, is more complex with the following three conceivable paths:

(i) *A typical A2 mechanism*

This reaction path corresponds to that of the A2 hydrolysis of acetamide and methyl carbamate reported previously; the N-protonated form (VII) is attacked by water in the rate determining step with a tetrahedral TS (TS 1).<sup>19</sup> The MNDO activation barrier was 49.74 kcal/mol, which is again the highest among the similar processes in acetamide (44.16 kcal/mol) and methyl carbamate (46.92 kcal/mol). The MNDO potential energy profile and the optimized geometries are given in Figures 10 and 11. This A2 hydrolysis of the N-protonated urea, however, has the lower activation barrier by 10.09 kcal/mol than that of the O-protonated form.

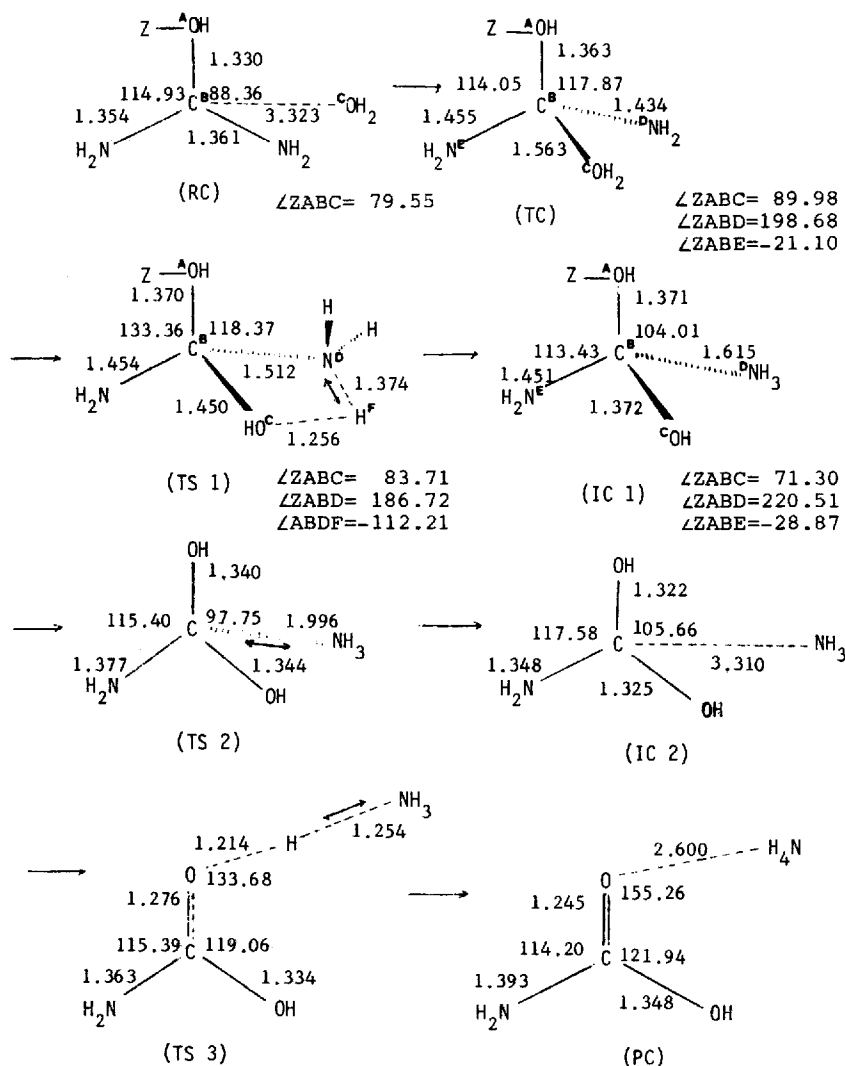
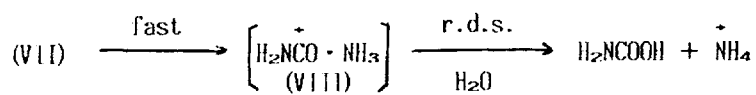


Figure 8. Geometries for the stationary point species on the potential energy profile for the A2 hydrolysis of O-protonated tautomer, (VI). The double headed arrow ( $\leftrightarrow$ ) indicates a reaction coordinate, the dihedral angle is represented with the  $LWXYZ$  and the  $Z$  is a dummy atom (bond lengths and angles are in Å and degree)

(ii) *An ion-pair like  $S_N2$  mechanism*<sup>20</sup>

In this process, the  $\text{NH}_3$  group is expelled first from the N-protonated form (VII) forming an ion-pair like complex (VIII), and subsequently water reacts with  $\text{H}_2\text{NCO}^+$  in a rate determining nucleophilic attack on the carbonyl carbon as in Scheme 5. The MNDO potential energy profile and optimized geometries are presented in Figures 12 and 13. Examination of these Figures reveals that the process following IC 2 are exactly the same as the process after IC 1 in the A2 hydrolysis of the N-protonated form in Figure 10. The MNDO activation barrier in this mechanism, 45.31 kcal/mol, is lower by 4.44 and 14.52 kcal/mol than those of the



Scheme 5

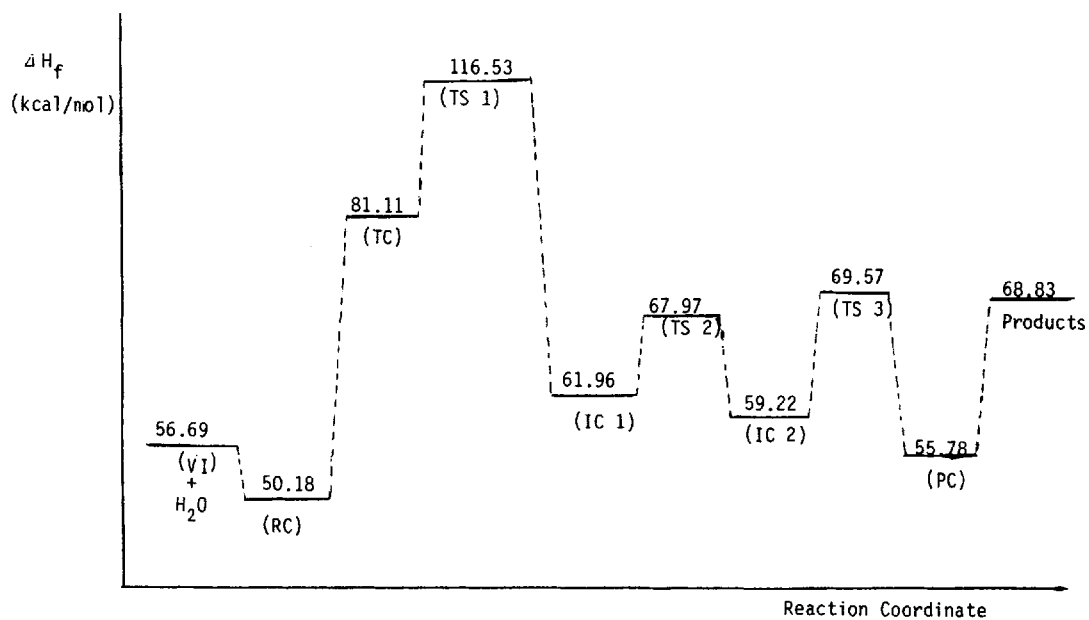


Figure 9. Potential energy profile for the A2 hydrolysis of O-protonated tautomer, (IV)

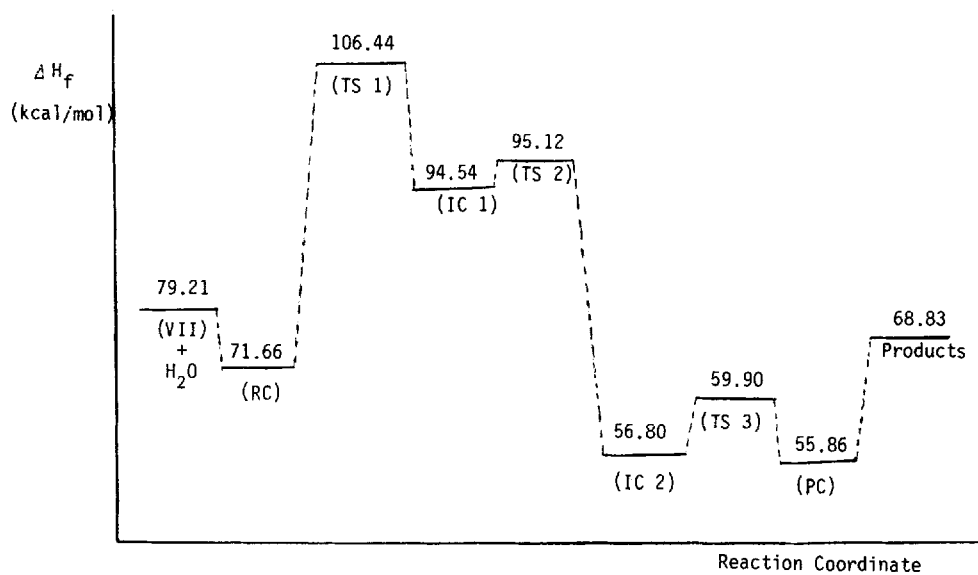


Figure 10. Potential energy profile for the A2 hydrolysis of N-protonated tautomer, (VII)

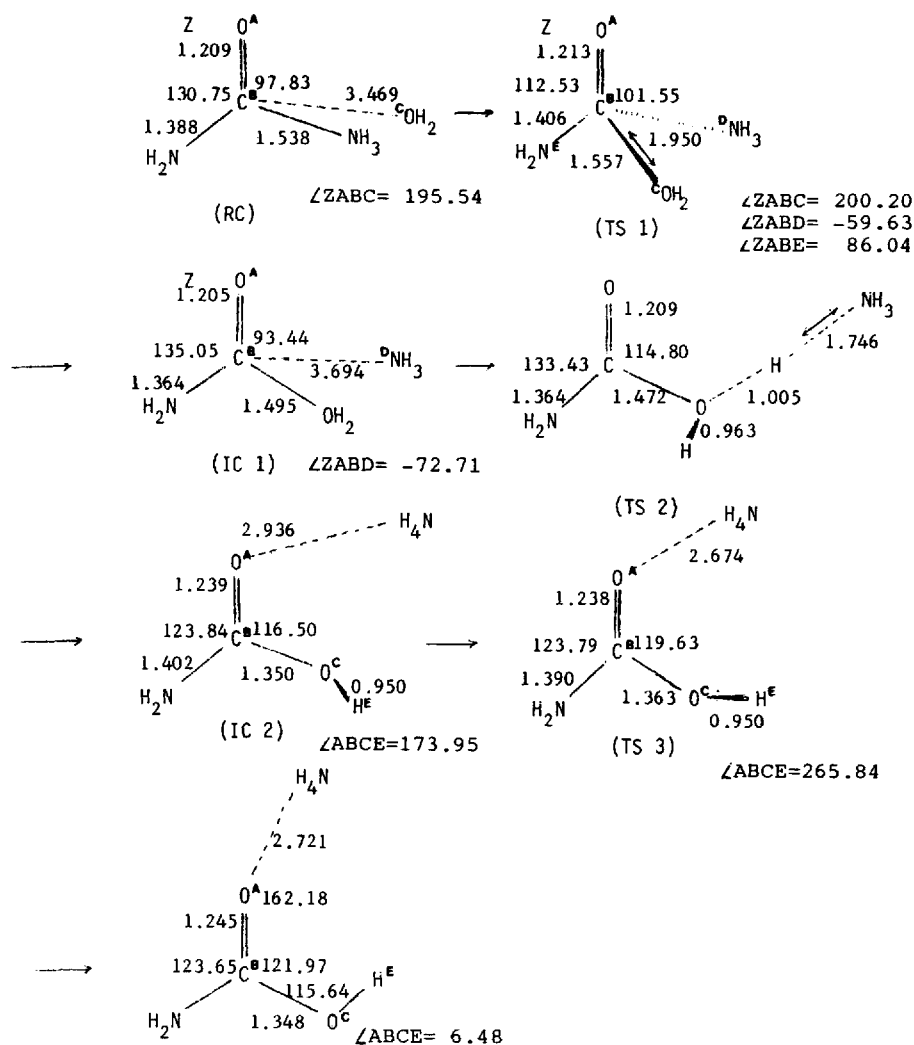


Figure 11. Geometries for the stationary point species on the potential energy profile for the A2 hydrolysis of N-protonated tautomer, (VII). The double headed arrow ( $\leftrightarrow$ ) indicates a reaction coordinate, the dihedral angle is represented with the  $\angle WXYZ$  and the Z is a dummy atom (bond lengths and angles are in Å and degree)

A2 hydrolysis of the N-protonated and O-protonated tautomers, respectively. Therefore this ion-pair like  $S_N2$  path is the most preferred one among all those conceivable for the A2 hydrolysis of the monoprotonated urea.

### (iii) An A1 decomposition with water as a hydrogen transfer agent

In the mechanism proposed by Giffney *et al.*,<sup>4</sup> the N-protonated tautomer (VII) forms a hydrogen bonded, six-membered cyclic complex with one water molecule (IV), which undergoes a rate determining decomposition (Scheme 2). However, we have failed to obtain a

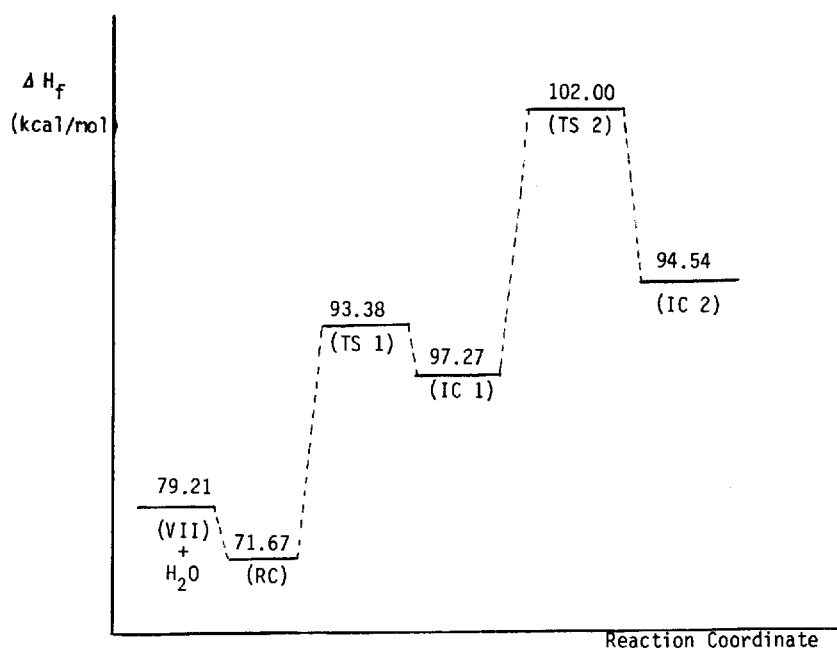


Figure 12. Potential energy profile for the ion-pair like  $S_N2$  hydrolysis of N-protonated tautomer, (VII)

(RC ; same structure with (RC) in Figure 11)  $\longrightarrow$

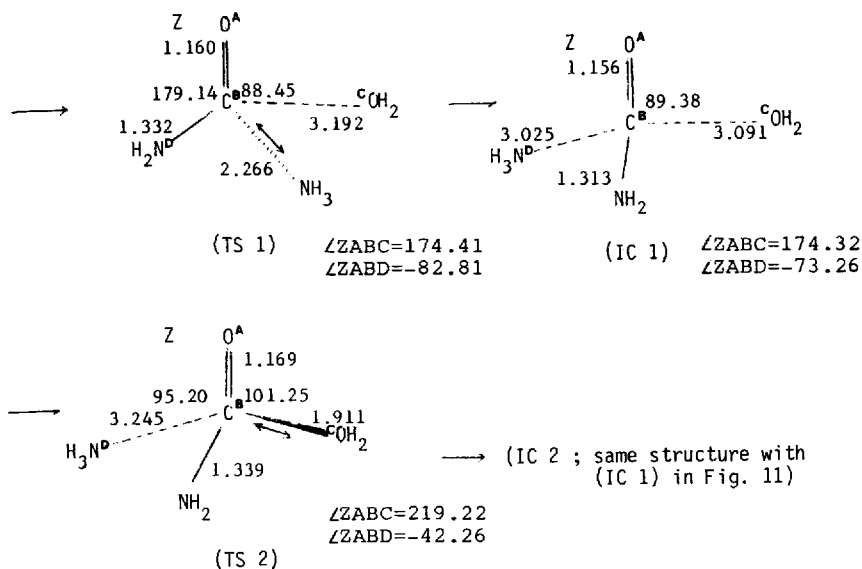


Figure 13. Some geometries for the stationary point species on the potential energy profile for the ion-pair like  $S_N2$  hydrolysis of N-protonated tautomer. The double headed arrow ( $\longleftrightarrow$ ) indicates a reaction coordinate, the dihedral angle is represented with the  $LWXYZ$  and the  $Z$  is a dummy atom (bond lengths and angles are in Å and degree)

stationary structure corresponding to the stable cyclic six-membered ring complex (IV); the species was non-existent either as an equilibrium species or as a TS both by the MNDO and the AM1 method of computations. This is understandable in view of the localized ammonium type cationic center in the complex (IV); the localized cationic center makes it even more difficult to form a stable hydrogen bonded cyclic complex than in the free base form, (III), with the neutral center, and makes bond breaking of the  $\text{—NH}_3^+$  group much easier in the TS so that it will give a TS which is similar to the one in the ion-pair like  $\text{S}_\text{N}2$  mechanism above.

An overview of the activation barriers involved in the hydrolysis of the monoprotonated urea is illustrated in Figure 14.

### Hydrolysis of the diprotonated form

Moodie *et al.*<sup>3b</sup> have observed a shallow maximum in the acid hydrolysis rate of urea at *ca.* 70% w/w  $\text{H}_2\text{SO}_4$ , which has been attributed to the common A2 hydrolysis of the diprotonated form. The MNDO activation energy for this process was found to be lower by 26.09 kcal/mol than that for the monoprotonated species. Urea has been shown to be fully diprotonated in the very highly acidic media by Olah *et al.*,<sup>21</sup> and evidence of about 10% diprotonation in the case of NNN'N'-tetramethylurea has been reported by Gillespie *et al.*<sup>22</sup> We were able to obtain a fully optimized structure for the diprotonated urea, in agreement with the experimental findings. The MNDO potential energy profile and the optimized geometries involved in the hydrolysis of the diprotonated urea are presented in Figures 15 and 16. Inspection of Figure

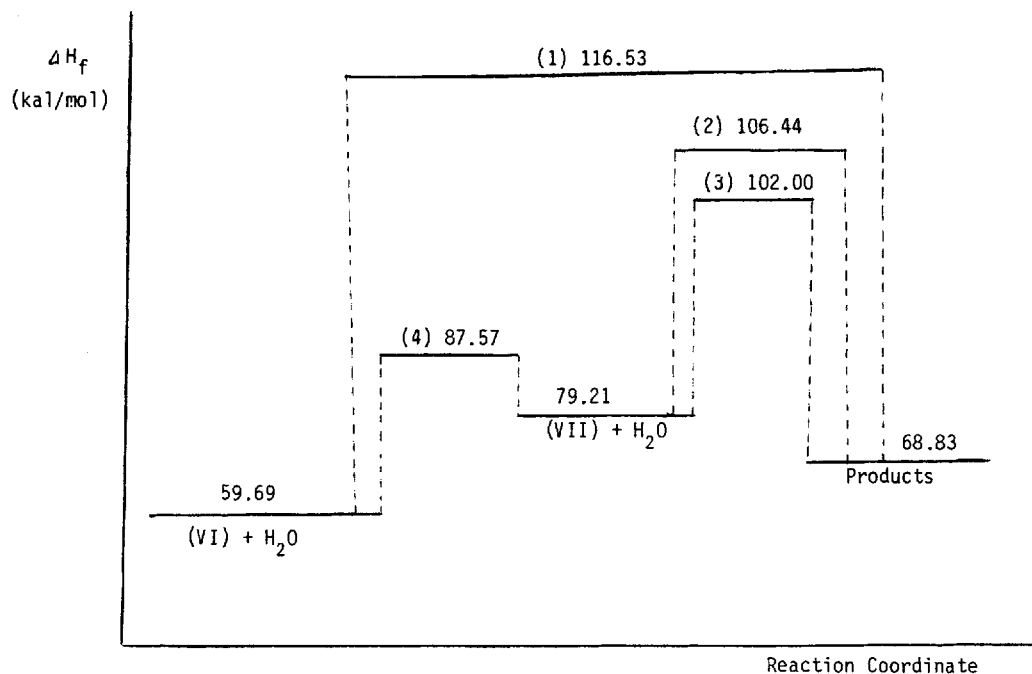


Figure 14. An overview of activation barriers involving acid hydrolysis of monoprotonated urea. (1) is an A2 hydrolysis path of O-protonated tautomer, (2) is an A2 hydrolysis path of N-protonated tautomer, (3) is an ion-pair like  $\text{S}_\text{N}2$  hydrolysis path of N-protonated tautomer and (4) is a solvated proton transfer process,  $(\text{VI}) + \text{H}_2\text{O} \rightarrow (\text{VII}) + \text{H}_2\text{O}$

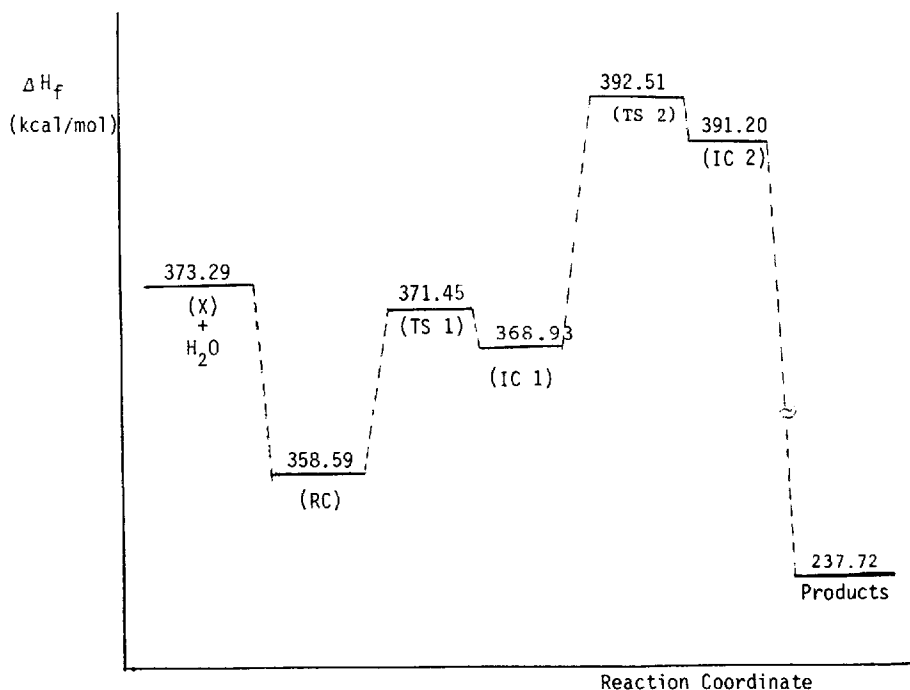


Figure 15. Potential energy profile for the acid hydrolysis of diprotonated urea, (X)

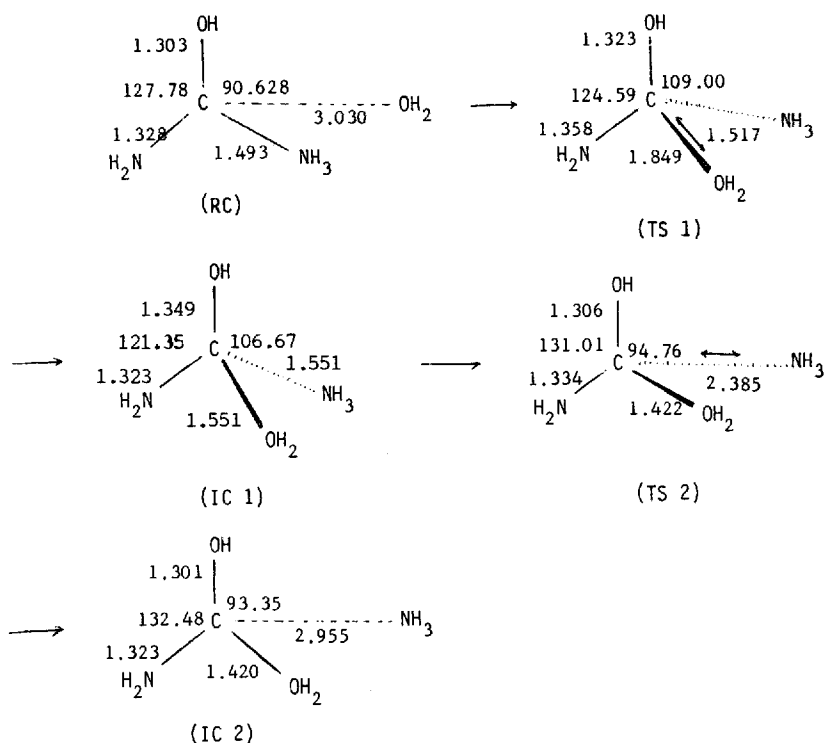
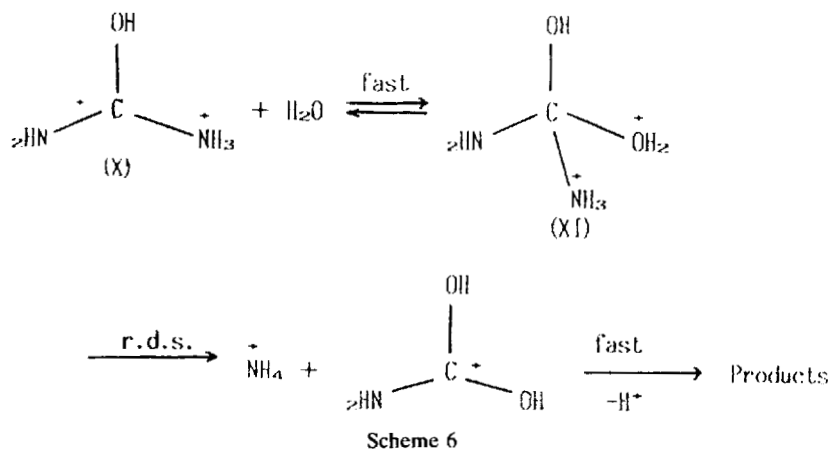


Figure 16. Geometries for the stationary point species on the potential energy profile for the acid hydrolysis of diprotonated urea. The double headed arrow indicates a reaction coordinate (bond lengths and angles are in Å and degree)

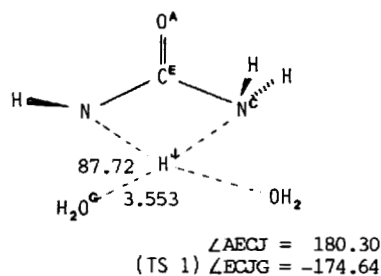
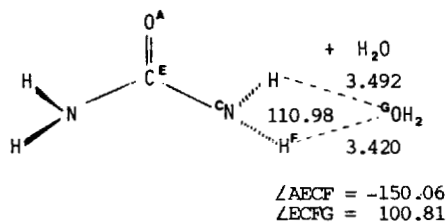
15 shows that the rate determining step in this path is the expulsion of  $\text{NH}_3$  (TS 2) from the tetrahedral intermediate<sup>22</sup> XI, which was formed in the nucleophilic attack of the diprotonated form X by water (Scheme 6).



The MNDO activation barrier was found to be 19.22 kcal/mol, which agrees approximately with the solution phase experimental value in this case. Activation energy for the hydrolysis of

(A) Neutral Urea

a) One solvate water molecule



b) Two solvate water molecules

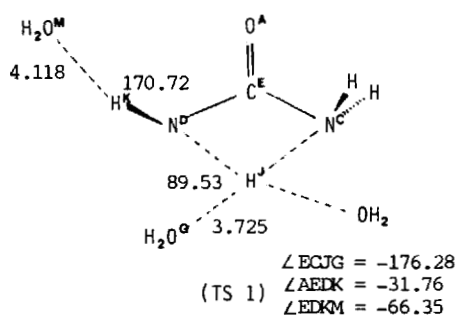
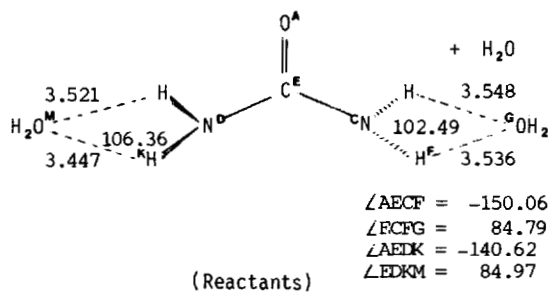


Figure 17.



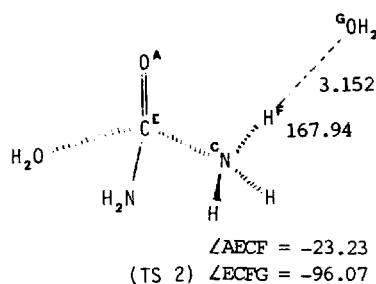
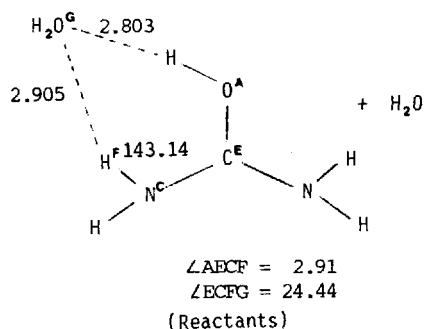
ethylurea in 79.9% w/w  $\text{H}_2\text{SO}_4$  solution has been reported to be 23.7 kcal/mol.<sup>3b</sup> The products formed after the TS 2 are the two monoprotonated species,  $\text{NH}_4^+$  and  ${}^2\text{HNC}(\text{OH})_2^+$ , which have much lower heats of formation,  $\Delta H_f$ , providing further driving force for the facile hydrolysis of the diprotonated form.

Results of our theoretical investigation can be summarized as follows: (i) For the unprotonated urea, decomposition path involving intramolecular hydrogen transfer of N-bound hydrogen is preferred either to the direct hydrolysis by the attack of water on the carbonyl carbon or to the intermolecular decomposition path with a water as the hydrogen transfer agent; (ii) For the monoprotonated urea, an ion-pair like  $\text{S}_\text{N}2$  mechanism involving the N-protonated form provides the lowest barrier path in the hydrolysis; (iii) The A2 hydrolysis of the diprotonated urea is preferred to that of the monoprotonated species; (iv) The hydrolysis of the monoprotonated species is favored over that of the unimolecular decomposition path of the unprotonated species.

Figure 17. (continued)

(B) Monoprotonated Urea

a) One solvate water molecule



b) Two solvate water molecules

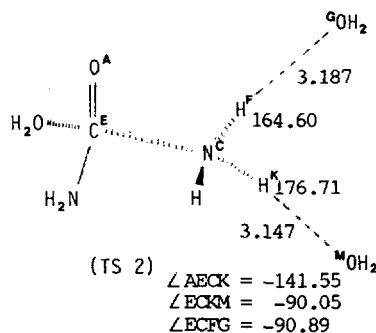
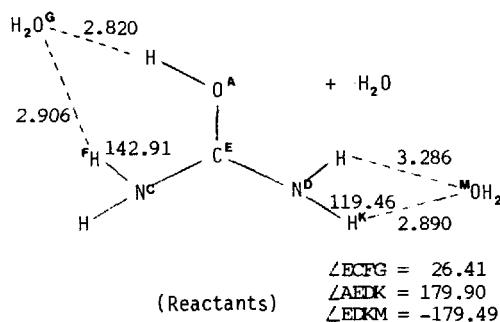


Figure 17. Conformations of the solvate water molecules. The dihedral angle is represented with the LWXYZ (bond lengths and angles are in Å and degree)

### Solvation effect

The results (i)–(iii) are consistent with the conclusions reached experimentally by Moodie *et al.*<sup>3</sup> However, the result (iv) is in direct conflict with the experimental findings that the unimolecular decomposition path is preferred to the hydrolysis of the monoprotonated species in the relatively low acidity range.

In view of the fact that our theoretical studies are based on the gas phase reactions, this conflict may be resolved by considering solvation effect, which should certainly have dominant influence on the activation barriers in solution phase reactions involving ionic reactants. In order to account for such effect of solvation, we have carried out calculations of barrier heights for the unimolecular decomposition and the ion-pair like  $S_N2$  paths by including up to two solvate water molecules both in the ground and transition states. The conformations of the solvate water molecules are presented in Figure 17. Our MNDO results are summarized in Table 1. We note in this Table that as the number of water molecules ( $n$ ) increases,  $n = 0$ –2, the activation barrier for the A2 hydrolysis increases in a greater rate compared with that for the decomposition path. Thus if we were to extend this type of computation further to a large number of solvate water molecules, the trends may well be reversed in favor of the neutral unimolecular decomposition path. Admittedly this study involves too small a number of solvate molecules and the extrapolation seems too far-fetched. However the qualitative trends are clear: for the neutral decomposition, partial charge separation in the TS increases intermolecular force due to dipole–dipole interaction between substrate and solvate water stabilizing the TS more relative to the neutral ground state, whereas for the A2 hydrolysis of the N-protonated species positive charge on N delocalizes in the TS so that preferential solvation of the ground state by ion–dipole interaction relative to the charge delocalized TS leads to an increase in the activation barrier. Moreover inclusion of hydrogen-bond effects, which was not accounted for in the MNDO methods<sup>8</sup> in our calculations above, should intensify the trends in elevating the barrier for the A2 path relative to the neutral decomposition. We therefore conclude that in solution phase, the neutral decomposition mechanism may well become the favored path over the A2 hydrolysis of the monoprotonated species. Thus our MNDO results are able to accommodate all experimentally postulated mechanisms by Shaw *et al.* and Moodie *et al.*, but do not support the six-membered cyclic mechanism of Giffney *et al.* The activation barriers calculated in these studies are certainly too

Table 1. Solvation effect for the activation barrier differences between the intramolecular decomposition process of neutral urea and an ion-pair like  $S_N2$  hydrolysis process of monoprotonated urea

$n^a$	Activation barrier of neutral urea ( $\Delta\Delta H_f(U)$ )	Activation barrier of monoprotonated urea ( $\Delta\Delta H_f(UH^+)$ )	$\Delta(\Delta\Delta H_f)^b$
0	71.17 <sup>c</sup>	45.31	25.86
1	71.39	49.09	22.30
2	71.53	51.17	21.36

<sup>a</sup>Number of solvate water molecule.

<sup>b</sup> $\Delta(\Delta\Delta H_f) = \Delta\Delta H_f(U) - \Delta\Delta H_f(UH^+)$ .

<sup>c</sup>kcal/mol.

high due to a well-known weakness of the MNDO method.<sup>8,17</sup> Even though the absolute values of barrier heights may be unrealistic, the relative values have been useful in the elucidation of mechanistic features.<sup>23</sup> As to the common mechanism for the A2 hydrolysis of amides, carbamates and ureas, we must conclude that ureas do not react via the common mechanism which was found for the other two compounds.

## ACKNOWLEDGEMENTS

We thank the Korea Science and Engineering Foundation and the Ministry of Education for support of this work.

## REFERENCES

1. Part 55 of the series: Determination of Reactivity by MO Theory.
2. (a) W. H. R. Shaw and J. J. Bordeaux, *J. Am. Chem. Soc.*, **77**, 4729 (1955); (b) W. H. R. Shaw and D. G. Walker, *J. Am. Chem. Soc.*, **79**, 4329 (1957); (c) W. H. R. Shaw and D. G. Walker, *J. Am. Chem. Soc.*, **80**, 5337 (1958).
3. (a) V. C. Armstrong, D. W. Farlow and R. B. Moodie, *J. Chem. Soc., (B)*, 1099 (1968); (b) D. W. Farlow and R. B. Moodie, *J. Chem. Soc., (B)*, 407, (1971).
4. J. Giffney and C. J. O'Connor, *J. Chem. Soc., Perkin Trans. 2*, 362 (1976).
5. I. Lee, C. K. Kim and H. S. Seo, *Tetrahedron*, **42**, 6627 (1986).
6. I. Lee, C. K. Kim and B. C. Lee, *J. Comput. Chem.*, **8**, 794 (1987).
7. M. J. S. Dewar and W. Thiel, *J. Am. Chem. Soc.*, **99**, 4899 (1977).
8. M. J. S. Dewar, E. G. Zoebisch, E. F. Healy and J. J. P. Stewart, *J. Am. Chem. Soc.*, **107**, 3902 (1985).
9. (a) Available from Quantum Chemistry Program Exchange (QCPE), No. 353; (b) Available from Quantum Chemistry Program Exchange (QCPE), No. 506.
10. (a) K. Muller, *Angew. Chem. Int. Ed. Engl.*, **19**, 1 (1980); S. Bell and J. S. Crighton, *J. Chem. Phys.*, **80**, 2464 (1984).
11. (a) A. Kormonichi, K. Ishida and K. Morokuma, *Chem. Phys. Lett.*, **45**, 595 (1979); (b) J. W. McIver, Jr. and A. Kormonichi, *J. Am. Chem. Soc.*, **94**, 2025 (1972).
12. I. G. Csizmadia, *Theory and Practice of MO calculations on Organic Molecules*, Elsevier, Amsterdam, 1976, p. 237.
13. (a) F. M. Menger, J. Grossman and D. C. Liotta, *J. Org. Chem.*, **48**, 905 (1983); (b) K. Yamashita, M. Kaminoyama, T. Yamabe and K. Fukui, *Theoret. Chim. Acta*, **60**, 303 (1981); I. Lee, J. K. Cho and B.-S. Lee, *J. Comput. Chem.*, **5**, 217 (1984).
14. W. J. Svribely and J. C. Werner, *J. Am. Chem. Soc.*, **57**, 1983 (1935).
15. J. W. Moore and R. G. Pearson, *Kinetics and Mechanism*, 3rd Ed., Wiley, New York, 1981, p. 266.
16. I. Lee, C. K. Kim, B.-S. Lee and S. C. Kim, *Tetrahedron*, In press.
17. W. Thiel, *J. Am. Chem. Soc.*, **103**, 1420 (1981).
18. I. Lee, C. K. Kim and H. S. Seo, *Bull. Korean. Chem. Soc.*, **7**, 395 (1986).
19. (a) S. Yamabe and T. Minato, *J. Org. Chem.*, **48**, 2972 (1983); (b) O. I. Asubiojo and J. I. Brauman, *J. Am. Chem. Soc.*, **101**, 3715 (1979).
20. R. A. Y. Jones, *Physical and Mechanistic Organic Chemistry*, Cambridge Univ. Press, Cambridge, 1979, p. 129.
21. G. A. Olah and A. M. White, *J. Am. Chem. Soc.*, **90**, 6087 (1968).
22. T. Birchall, J. Gaudie and R. J. Gillespie, *Non-aqueous Solvent Systems*, Academic Press, New York, 1965, p. 191.
23. (a) M. J. S. Dewar and M. L. McKee, *J. Am. Chem. Soc.*, **100**, 7499 (1978); (b) M. J. S. Dewar, D. J. Nelson, P. B. Shevlin and K. A. Biesiada, *J. Am. Chem. Soc.*, **103**, 2802 (1981); (c) M. J. S. Dewar and L. Chantranupong, *J. Am. Chem. Soc.*, **105**, 7152 (1985); (d) F. Carrion and M. J. S. Dewar, *J. Am. Chem. Soc.*, **106**, 3531 (1984); (e) M. J. S. Dewar and D. R. Kuhn, *J. Am. Chem. Soc.*, **106**, 5256 (1984); (f) M. J. S. Dewar and K. M. Merz, *J. Am. Chem. Soc.*, **107**, 6111 (1985).